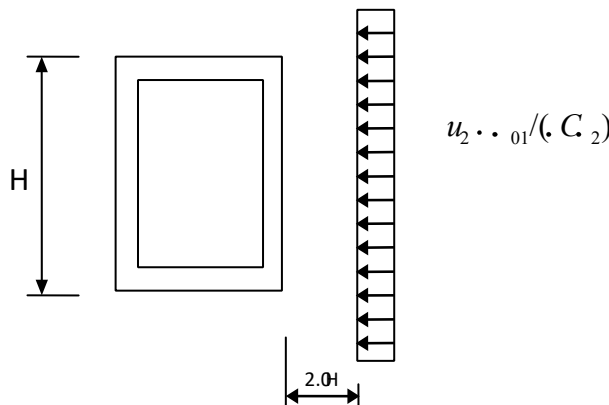


Where σ - amplitude of external loads; ρ - material plane; C – Speed of consideration of longitudinal waves. For non-stationary tasks, the principle of causality is required as the conditions for studying: in a medium there should be no displacements outside the region bounded by the leading edge of the waves coming from the oscillation sources. Boundary conditions on the boundary of the calculated region for fission dynamic (seismic) effects. When solving problems for infinite elements from an infinite half-plane, studies are made of the calculated domain of finite dimensions. The region under investigation is discretized, and it becomes necessary to set up such conditions on the boundary that would not manifest itself on the results of the solution due to reflection, which occurs with long-term dynamic influences. Some researchers propose to consider solutions only a certain distance from the boundary of the region [4.8], considering that the reflection of the wave does not have time to reach this site in the considered period of time. Sometimes it is advisable to introduce additional artificial damping into the calculation area, increasing as we approach the boundary [7]. In Lismer's paper, boundary conditions were proposed for a finite computational domain, allowing one to simulate an infinite medium. These boundary conditions pass the wave through the boundary of the calculated region without reflection, that is, the so-called standard viscous boundary is obtained. The tasks of the standard viscous boundary are carried out by replacing the reaction of the parts of the half-plane that are not pressed into account by distributed loads σ and τ , calculated formulas:

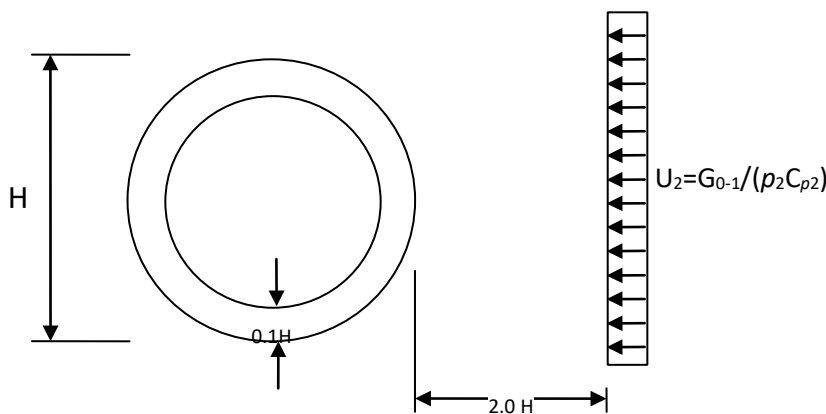
$$\sigma = -C_p u; \quad \tau = -C_s \dot{u}; \quad (3)$$

where u and \dot{u} - the velocity of the points on the boundary of the body, respectively, along the coordinates X_1 and X_2 . ρ and ρ - unlimited options; ρ - material density; C_p and C_s - the velocity of the longitudinal and transverse waves, respectively. Similar conditions can be considered as setting a viscous damper at the boundary.

6



B. The action of an elastic wave on a reinforced square hole



a.. The effect of an elastic wave on a reinforced circular hole

Fig.1. Calculation schemes.

Methods of solution. The FEM procedures provide for a transition from differential dependencies, for individual finite elements to a global system of equations for the entire array. For linear problems of nonstationary interaction, this system has the form [14]:

$$M \ddot{q} + S \dot{q} + K q = F + p \quad (4)$$

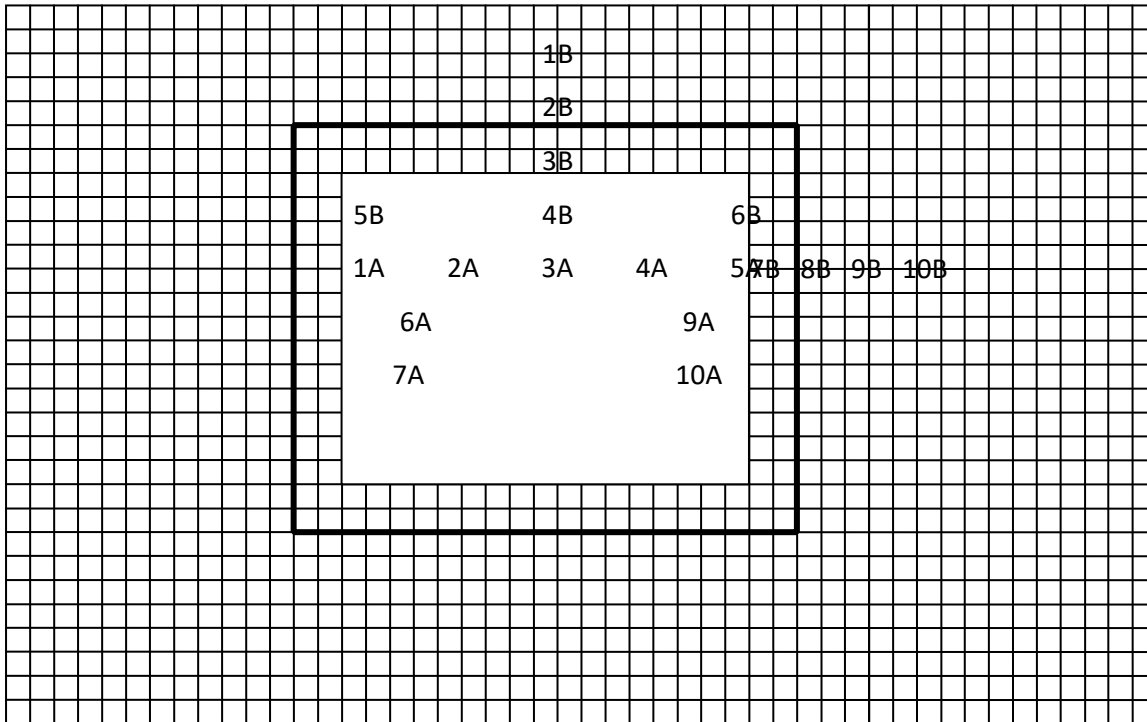


Fig. 2. Points in which elastic stresses are given in time.

here [M], [S], [K] – respectively, the matrices of the masses, the damping of the rigidity of the system; \ddot{q} , \dot{q} , q – vectors rooted, speed and displacement; {F} – vector external load; [p] – matrix of external damping. The matrix differential equation (4.4) in finite-difference form using the Newmark method [15]

$$[M] \ddot{q} + [S] \dot{q} + [K] q = F + p \quad (5)$$

where j, j+1, j+2 – past, present and future values of variables; β – parameter chosen from the conditions of numerical stability and accuracy. In this example, it is adopted $\beta = 1/4$. Thus, we obtain a system of linear algebraic equations, which is solved by a time step. By Proposition [15], the following relations were used to determine the displacement and velocity: $\{q\}^{j+1} = \{q\}^j + \{ \dot{q} \}^j + \frac{1}{2} \{ \ddot{q} \}^j$

$$\{q\}^{j+1} = \{q\}^j + \{ \dot{q} \}^j + \frac{1}{2} \{ \ddot{q} \}^j \quad (6)$$

where γ characterizes circuit damping $\gamma = 1/2$ at which there is no attenuation. The relation (5) can be represented in the form of an algebraic system $[A] \{q\}^{j+1} = \{R\}^j$

$$(7)$$

$$\{R\}^j \cdot \{F\}^j \cdot ([M] \frac{2}{(\Delta t)^2} \cdot [K]) \{q\}^j \cdot \{q\}^{j-1}; \frac{1}{(\Delta t)^2}$$

implement a typical procedure for calculating the variable vector $\cdot q(t)$.

Then, in the case of diagonal matrixes of elements' masses, the matrix of the system is also diagonal. The time integration step is assumed to be equal to $0,125 \cdot 10^{-4}$ with a minimum period of free oscillations of the element $6,28 \cdot 10^{-4}$ s.

The solution of the problem of the action of a plane longitudinal elastic wave on a circular cavity. In a rectangular Cartesian coordinate system, a plane region is considered in which a circular hole is defined (Fig. 1). The initial conditions are assumed to be zero, which corresponds to the absence of elastic displacements and velocities at $t = 0$. When $0 \cdot n \cdot 10$ ($n \cdot t/t$) The rate of elastic displacement and varies from 0 to $p \cdot \cdot / (pc_p)$, $\cdot \cdot \cdot 0,1$ (MPa), at $n \cdot 10 u = p$, which corresponds to the action of a plane longitudinal elastic wave of the Heaviside function type $\cdot 01$ (Fig.3)

$$\cdot \cdot \cdot 0 H(t), \quad (8)$$

$$1 \cdot v \quad \text{where} \quad t = t + (x+R)/c_p, \quad (\cdot 0$$

$\cdot 1MPa$); c_p - Velocity of the longitudinal wave; R is the radius of the hole. The calculations were carried out with the following initial data: $H = 2.0$ m;

$\Delta t = 0,407 \cdot 10^{-5}$ s; $E = 0,36 \cdot 10$ Mpa; $v = 0,36$; $p = 0,122 \cdot 10^4$ kg/m³; $c = 1841$ m/s;
 $n = t/\Delta t$.

Fig.3. Impact of the Heaviside function type

The investigated computational domain has 1536 nodal points. The contour of the round hole is approximated by 28 nodal points. The diameter of the circular aperture is the plane front of the action passing through $n = 24$. The graphs show that the numerical solution accurately reproduces the wave pattern. The discrepancy for the maximum compressive elastic contour stress σ_k is 6%. In Fig. 4 shows the variation of the elastic contour stress σ_k at points 1A-5A in time $t/\Delta t$, under the action of (8), the compressive elastic contour stress σ_k at point 1A increases to a maximum, and then, oscillating, asymptotically tends to a constant value. Multiple superposition of straight, reflected and diffracted elastic waves leads to a concentration of the compressive elastic contour stress σ_k in the neighborhood of the point 1A. The maximum value of the compressive elastic contour stress σ_k reaches at point 1A in almost three passes the front of the longitudinal wave of the diameter of the circular hole and is equal to $\sigma_k = -2,712$. The graphs show that the elastic stress state near the circular hole tends to the corresponding nominal elastic stresses.

The effect of an elastic wave on a reinforced circular hole.

In a rectangular Cartesian coordinate system, a plane region in which a free circular hole is defined is considered. We consider reinforcement with a ratio of the diameter of the middle contour to the thickness, equal to ten. The initial conditions are assumed to be zero, which corresponds to the absence of elastic displacements and velocities of elastic displacements at $t = 0$. In the cross section at a distance of 2.ON (Fig. 1) with $o \cdot n \cdot 10$ ($n \cdot t/t$) The velocity of elastic displacement and vary linearly from 0 to $p \cdot \cdot 0 / (\cdot 2c_{p2})$, $\cdot 0 \cdot \cdot 0,1$ Mpa (-1 kgs/sm), and for $n > 10 u = p$, which corresponds to the action of a plane longitudinal elastic wave of the Heaviside function type σ_0 The calculations were carried out with the following initial data: $H = 2.0$ m.

$\Delta t_1 = 0,186 \cdot 10^{-5}$ s ; $E_1 = 0,72 \cdot 10^5$ Mpa ($0,72 \cdot 10^6$ kg/sm); $v = 0,3$; $p_1 = 0,275 \cdot 10^4$ kg/m ($0,275 \cdot 10^5$ kg/s /sm); $c_{p1} = 536$ m/s; $\Delta t_2 = 0,407 \cdot 10^{-5}$ s; $E_2 = 0,36 \cdot 10$ Mpa ($0,36 \cdot 10$) *5 $v = 0,36$; $p_2 = 0,122 \cdot 10^4$ kg/m³ ($0,122 \cdot 10^{-5}$ kgs/sm⁴); $c_{p2} = 1841$ m/s;

(... 1 - reinforcement, ... 2 - environment). The investigated computational domain has 1536 nodal points. The inner contour of the reinforced round hole is approximated by 28 nodal points. The thickness of the reinforced is approximated by two nodal ones. The outer contour of the reinforced round hole is approximated by 32 nodal points. The diameter of the middle contour of a reinforced circular hole is the flat front of the impact passing through $n = 60$. Figure 5 shows the variation of the compressive elastic contour

stress $\sigma_x(\sigma_x \cdot \sigma_x / \cdot)$ At point 1A in time $t(t \cdot (c_{p2t})/H\%$. 1(-)-2(-- --) – The results of an analytical and numerical solution under the action of (8). The discrepancy for the maximum compressive elastic contour

stress σ_x constitute 16%.

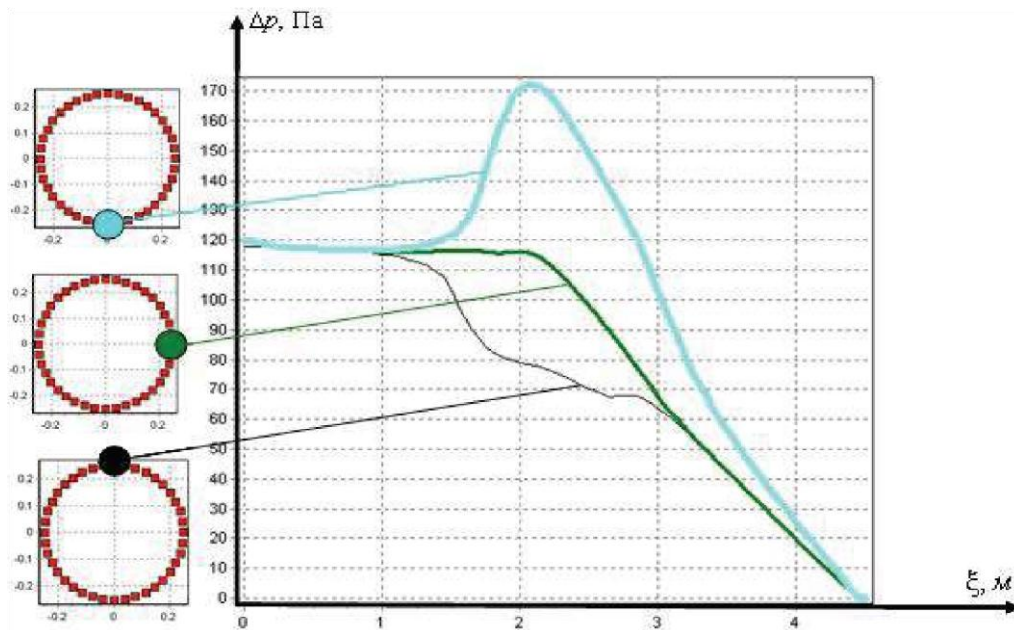


Figure 4. Pressure at various points in the pipeline

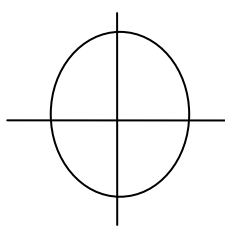
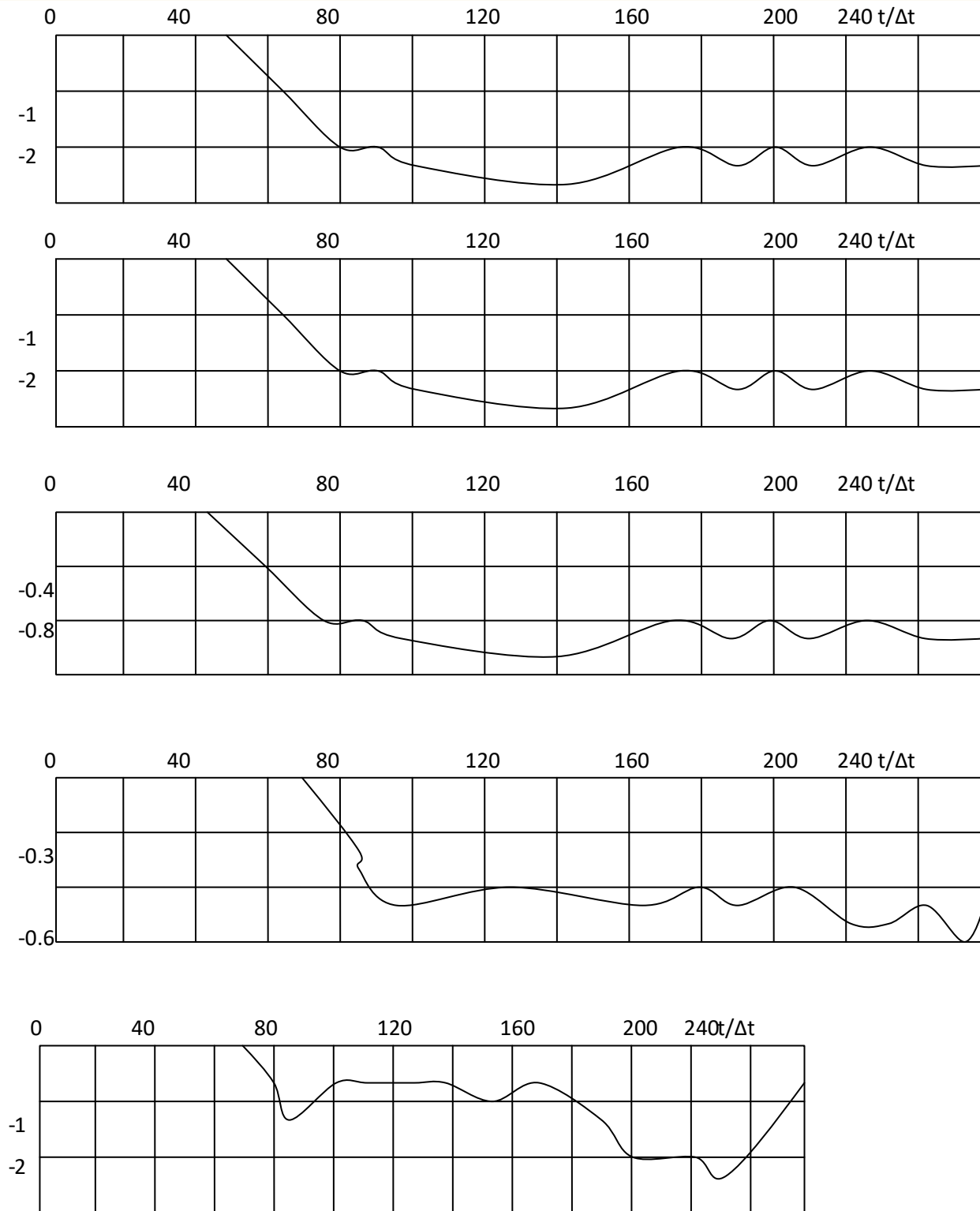


Fig.5. The change in the compressive elastic contour stress at points 1-5 in time $t/\Delta t$ on the contour of a free circular hole under the action of a plane longitudinal elastic wave of the Heaviside function type

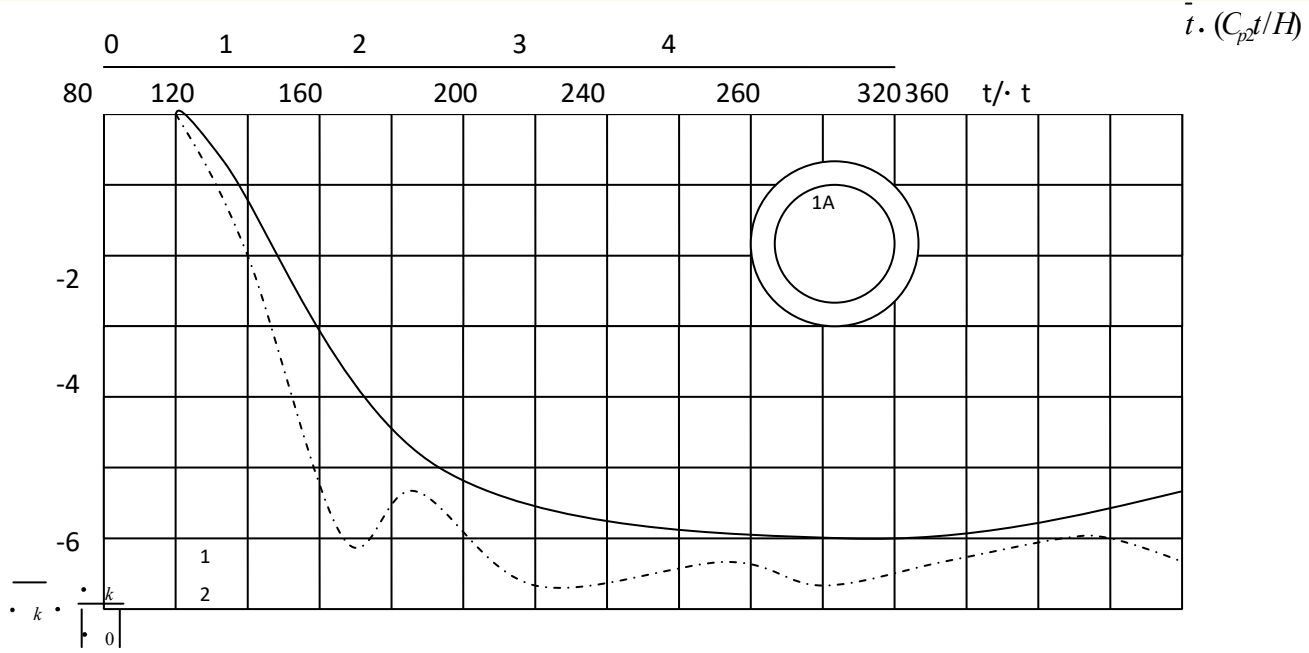
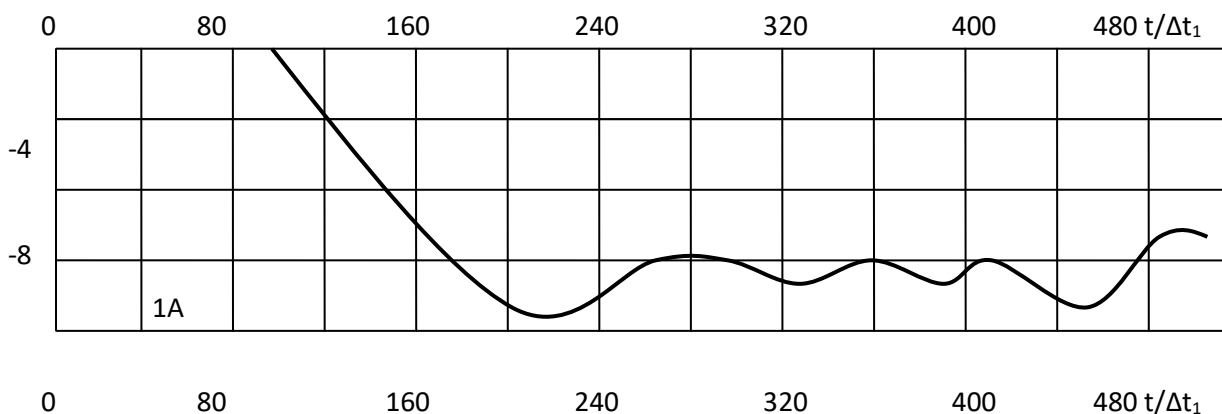


Fig. 6. The change in the compressive elastic contour stress σ_x at points 1A in time t on the contour of a free circular hole: 1-result of the analytical solution under the action of a flat longitudinal elastic wave of the Heaviside function type; 2-results of the numerical solution obtained by FEM in displacements under the action of a plane longitudinal elastic wave of the Heaviside function type.

The effect of a plane elastic wave on a reinforced square hole. We consider the problem of the interaction of a plane longitudinal elastic wave with a reinforced square hole. In a rectangular Cartesian coordinate system, a plane region in which a reinforced square hole is defined is considered. We consider reinforcement with the ratio of the side of the middle contour to a thickness of ten. The initial conditions are assumed to be zero, which corresponds to the absence of elastic displacements and velocities of elastic displacements at $t = 0$. In section by distances $0 \leq n \leq 10$ ($n = t/\Delta t$) the rate of elastic displacement and varies linearly from 0 to $P = \sigma_0 \cdot (\rho_2 c_{p2})$ ($\sigma_0 = -0,1 \text{ MPa}$ (-1 kgs.sm)), at $n > 10$ $u_2 = p$, Which corresponds to the action of a plane longitudinal elastic wave of the Heaviside function type (Fig. 3). The calculations were carried out with the following initial data: $H = 2,0$; $\Delta t = 0,186 \cdot 10^{-5} \text{ s}$; $E_1 = 0,72 \cdot 10^5 \text{ MPa}$ ($0,72 \cdot 10^6 \text{ kgs/sm}^2$); $\nu = 0,3$.



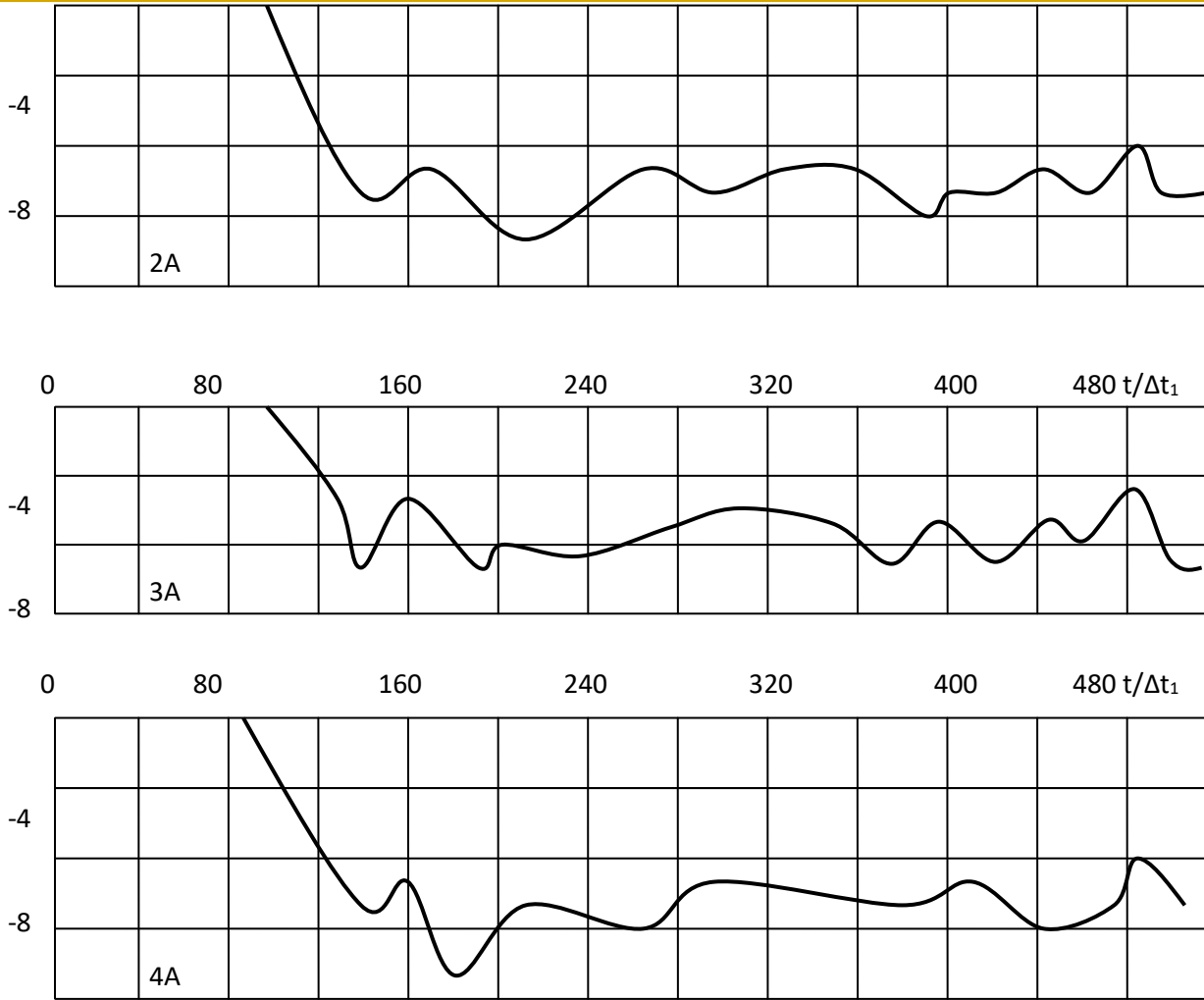
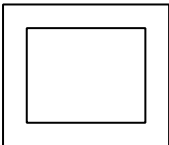


Fig.7. Changing the compressive contour $\bar{\nu}_k$ at points 1A-4A in time $t/\Delta t_1$ on the inner contour of the reinforced square hole under the action of a plane longitudinal elastic wave of the Heuside function type.



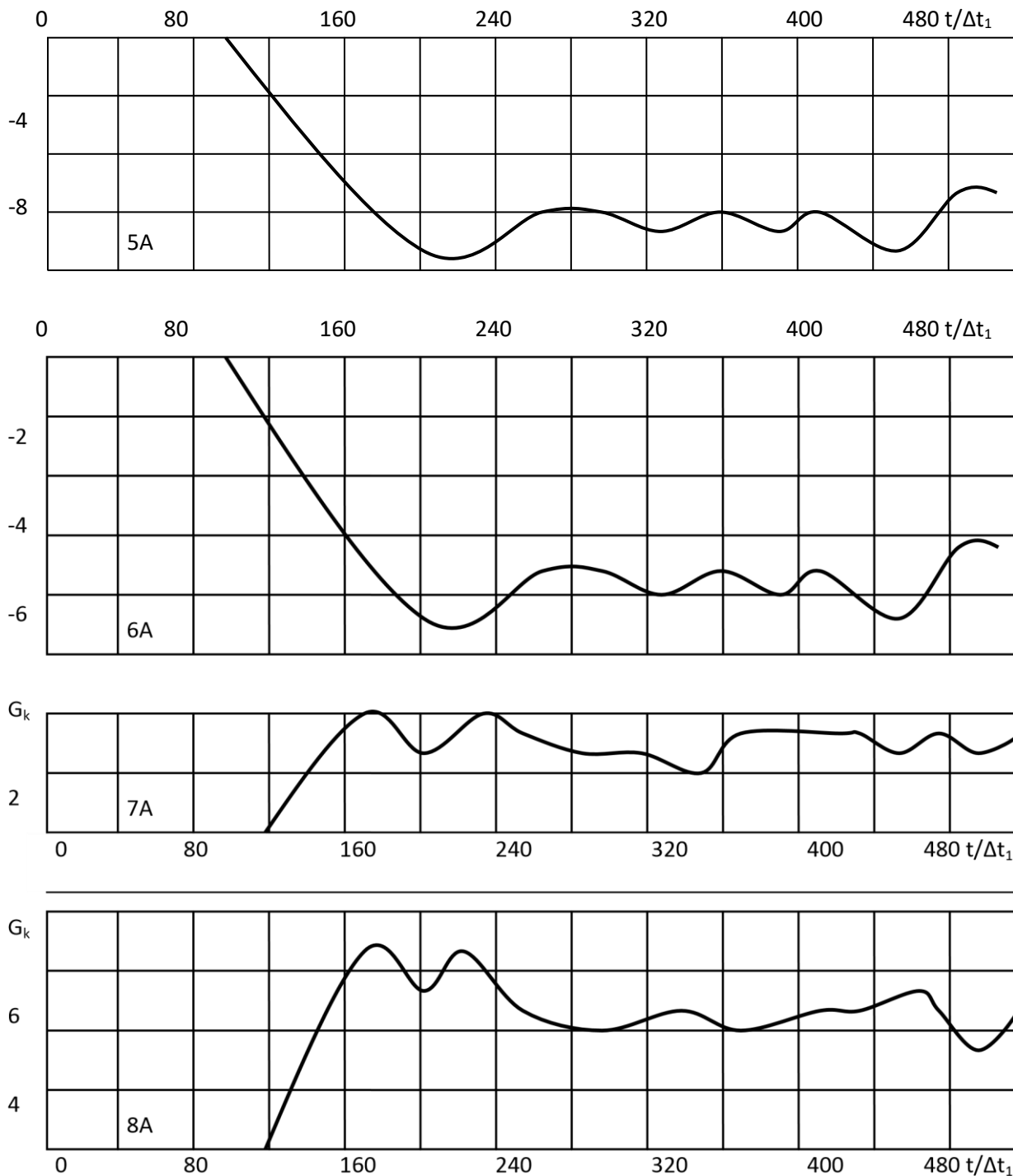
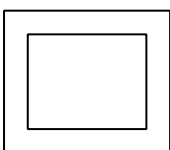


Fig. 8. Changing the loop voltage \cdot_k at points 5A-8A in time

6A 5A 7A $t/\cdot t_1$ on the inner contour of the reinforced square hole under the action 8A of a plane longitudinal elastic wave of the Heuside function type.



The investigated computational domain has 13-40 nodal points. The inner contour of the reinforced square hole is approximated by 36 nodal points. The outer contour of the reinforced square hole is approximated by 44 nodal points. The diameter of the middle contour of a reinforced circular hole is the plane front of the action passing through $n = 60$. Fig.7-8 shows the changes in the elastic contour stress σ_k ($\sigma_k = \sigma_k / \sigma_k$) at

points 1A to 11A in time $t/\Delta t$ under the influence of (4.8); Compressive elastic contour stress σ_k at the point 5A increases to a maximum, and then, oscillating, asymptotically tends to a constant value. The constant superposition of straight, reflected and diffracted elastic waves leads to a concentration of the compressive elastic contour stress σ_k in a neighborhood of the point 5A. The maximum value of the compressive elastic contour stress σ_k reaches at the point of almost two passes of the front longitudinal wave of the side of the middle contour of the reinforced square hole and is equal to $\sigma_k = -13.9$. The graphs show that a compressive elastic normal stress reinforcement compresses the concentration of elastic stresses near the hole. The elastic stress state at a distance from the reinforced square hole tends to the corresponding nominal elastic stresses. Comparative analysis of contour stresses of a non-supported and reinforced hole (point 1A).

Conclusions

- under the influence of a plane longitudinal wave of the Heaviside function type, the maximum tensile elastic stress of the contour stress arises: for a free hole at a point located on the axis of symmetry in the shadow region of the internal reinforcement contour; For a reinforced square hole at a point located on the axis of symmetry in the illuminated area of the internal reinforcement contour.
- when a plane longitudinal elastic wave of the Heaviside function type is applied to a free circular hole and a free square hole, the compressive elastic contour stress of maximum magnitude reaches no more than three passes of a wave of characteristic size.
- the analysis of numerical results shows that the IEC in displacements can be successfully used to solve a planar dynamic problem of the theory of elasticity and becomes competitive with other methods of the dynamic theory of elasticity. Conducted studies of convergence and stability, comparison of the results of the numerical solution of the plane dynamic problem of the theory of elasticity obtained by the FEM in displacements, with the results of analytical solutions, showed their good agreement, which allows us to conclude about the physical reliability of the results of the numerical solution of the plane dynamic elasticity problem obtained by the FEM in Movements.
- the maximum value of stress intensity in a rectangular structure interacting with the medium is achieved at the boundary, near the corner point and at internal points of the body.
- the maximum contour stresses in the reinforced holes are four times greater than the maximum contour stresses in the free holes. The presence of reinforcement reduces the concentration of stresses in the medium.
- it is established that in the beginning the reinforced holes and by the time when the wave pass near its radii becomes almost uniformly comprehensively compressed, then a qualitatively new phase of motion occurs, at which the contour stresses are applied and the appearing appreciable flexural stresses are rapidly growing with the formation of five holes on the ring.

List of references

1. Guz A.N., Kubenko V.D., Cherevenko M.A.. Diffraction of elastic waves. Nauk, 1978. 308 p.
2. Pao Y.H., Mow C.C. diffraction of elastic waves and dynamic stress concentration. №4, Grane, Russak, 1973 694 p.
3. Ainbinder, A.B. Calculation of main and field pipelines for strength and stability: reference manual. M.: Nedra, 1991. - 287 p.
4. Shabrov N.N. Finite Element Method in Calculating the Details of Heat Engines. L.: Mechanical Engineering, 1983. - 212 p.
5. Mubarikov Ya.N., Safarov I.I. On the action of an elastic wave on a cylindrical shell. Series of engineering sciences, 1987. №4. from. 34-40
6. Safarov I.I. Estimation of the seismic stress of underground structures of the wave dynamics method Collection "Seismodynamics of tasks and structures" Tashkent, Ph. 1988.

7. L.A. Rozin, Fundamentals of the finite element method in the theory of elasticity. L. : Izd-vo LPI, 1972. 77 p.
8. Safarov I.I. Interaction of waves in multilayered cylindrical layers in an infinite elastic medium. Proceedings of VII All Union. Conference "Basic Dynamics, Foundations and Underground Structures" Dnepropetrovsk, 1989. p. 56-57
9. Safarov I.I., Zhumaev Z.F. On the destruction of the tunnel with strong movements of the earth. International Conference on Earthquake Engineering. S-Petrburg, 2000, p. 71-78
10. Avliyakov N.N., Safarov I.I. Modern problems of statics and dynamics of underground pipelines. Tashkent, Fan va texnologiya. 2007. 306 pp.
11. Yavarov A.V.. Numerical modeling of soil mass resistance to movements of an underground pipeline, in: Electronic Scientific Journal "Oil and Gas Business". 2012. № 3. Pp. 360-374.
12. Rashidov T.R., Safarov I.I. And others. Two main methods for studying the seismic stress of underground structures under the action of seismic waves. Tashkent: DAN. № 6, 1989. p 13-17.
13. Safarov I.I. Avliyakov N.N. Methods of increasing the seismic resistance of underground plastic pipelines // Uzbek Journal of Oil and Gas, 2005, No. 4.P.42-44.
14. Borodavkin, PP Underground main pipelines. - M. : Nedra, 1982. - 324 p.